Bulletin of the Institute of Mathematics
Academia Sinica (New Series)
Vol. **2** (2007), No. 2, pp. 587-607

BIFURCATION ANALYSIS OF A CLASS OF 'CAR FOLLOWING' TRAFFIC MODELS II: VARIABLE REACTION TIMES AND AGGRESSIVE DRIVERS

BY

I. GASSER, T. SEIDEL, G. SIRITO AND B. WERNER

Abstract

In this paper we continue the bifurcation analysis on follow-the-leader traffic models started in [6]. Two new aspects are included in the model: variable reaction time and aggressiveness of the drivers. Variable reaction time changes especially the periodic dynamics in the model. We show that more aggressiveness has a stabilizing effect on the traffic flow.

1. Introduction

In the second half of the last century many different approaches to describe vehicular traffic have been undertaken. The first paper in this context is due to Lighthill [17]. For an overview on the huge traffic flow literature see [9, 10, 15]. In the fifties so called microscopic traffic models came up, i.e. models where the dynamics of every single car is described (the first papers were [22, 23]). A special class are the so called follow-the-leader models, where the dynamics of every car depends mainly on its distance to the car in front (called headway) and on the relative velocity with respect to the car in front. A historical overview on follow-the-leader models is given in [4].

Considering such models on a circular road leads to an (in general big) autonomous system of ODE's. These systems are known to have special (quasi stationary) solutions with constant headways and constant relative

Received December 12, 2004 and in revised form May 2, 2005.
Key words and phrases: Hopf bifurcation, numerical continuation, traffic.

velocities. It is known that these solutions are stable up to a critical car-density [2, 11]. Especially in the last years there is a increased interest in the behavior beyond the critical density, i.e. in the region, where the quasi-stationary solution is unstable. A natural way to explore the dynamics beyond the critical density is bifurcation theory. In fact, a few authors based on numerical experiment have conjectured the existence of bifurcations [1, 13].

In [6] a systematic bifurcation analysis of standard optimal velocity models was presented. Here we investigate an extension of the model in two directions: on one hand we consider non-constant reaction times and on the other we include aggressive behavior. The main issue here is to study the influence of these two extensions on the dynamics.

At this point we should mention that similar bifurcation phenomena occur in related microscopic traffic flow models. In [12] a model for a bus route is considered and stability and bifurcation questions are studied. In [21] a bifurcation analysis of a model with delay for cars on a circular road is analyzed.

Consider the following system of ordinary differential equations describing N cars moving on a ring of given length L (quantities are already dimensionless):

$$\ddot{x}_j = \frac{1}{T\big(x_{j+1}-x_j\big)}\Big\{V\big(x_{j+1}-x_j\big)-\dot{x}_j+\alpha\cdot(\dot{x}_{j+1}-\dot{x}_j)F\big(x_{j+1}-x_j\big)\Big\}, \quad (1)$$

where $j = 1, \ldots, N$ and $x_j(t)$ is the distance of car j from a given origin with the prescription $x_{N+1} := x_1 + L$.

The function T has the meaning of a reaction time for the car-drivers' system. Its dependence on the headway should enable to mimic the fact that in a denser traffic situation drivers tend to be more alert and react faster than they do when in a relatively empty road. Accordingly T should be a positively valued function which monotonically increases with the headway and eventually saturates to a reaction time value of minimal alert.

Aside from the reaction time, the acceleration in system (1) is composed of two parts, describing two different but possibly coexisting driving behaviors. The first two terms correspond to the usual law prescribed in car following traffic models (see for example [2, 6, 10, 13, 19]. It states that car j tries to match its velocity to an optimal velocity given by function V in

terms of the headway. V will be taken such that V is positively valued and monotonically increasing with its argument, $V(0) = 0$, $\lim_{x\to\infty} V(x) = V_{max}$ (const.) and $V(x)$ is S-shaped, i.e., there exists a positive constant b such that $V''(x) > 0 \quad (< 0)$ if $x < b \quad (> b)$. Qualitatively different optimal velocity functions are involved in the case of car-bus systems (see [12]) or in the case of multi-lane traffic (see [14]).

The third term on the right hand side of (1) describes a more *aggressive* driving behavior, in that cars try to match the velocity of the car ahead of them. This tendency has been empirically observed and its definitely more marked when cars are driving near to each other, while, when headways grow, drivers tend to care less for what other drivers are doing. Function F is thus taken to be positive defined and decreasing in the headway. The coefficient $\alpha \in [0, \infty)$ is a *switch*, allowing to choose how much *aggressiveness* the drivers have.

In principle the parameter α and the functions V, T and F could all be taken to be different for each driver. This case will not be analyzed here. We thus make the hypothesis that all cars behave according to the same general law.

Historically the optimal velocity part of model (1) was introduced in [3] while the other part is much older and goes back to the fifties ([7]).

A further remark about equation (1) is that it is unable to deal with car-crashes and overtakings in a reasonable way. This means that headways $x_{j+1} - x_j$ can become negative without warning. When this happens, the dynamics doesn't reflect the new ordering of the cars and it is clear that the real world situation is not properly described any more. Moreover one cannot exclude the presence of solutions for which the velocities become negative. We call such solutions as *unphysical*. In the following, alongside the stability of solutions, we have to deal with their physicality too. Note though that we don't regard unphysical solutions as a failure of the model, we just have to be aware of their presence. An interesting approach to be found in literature is that of finding appropriate conditions on the initial data so as to prevent unphysical results (see for ex. [8]).

In this article we study the type of solutions of system (1) and their stability both analytically and with numerical simulations using the continuation algorithm AUTO2000 (see [5]). Section 1 deals with linear and

local bifurcation analysis of system (1), while in section 2 we perform the corresponding numerical bifurcation analysis.

2. Linear and Local Bifurcation Analysis

It is convenient to rewrite system (1) with respect to the variables $\phi_j = x_{j+1} - x_j$ and $\psi_j = \dot{x}_j$ with the prescription $\psi_{N+1} := \psi_1$

$$\begin{cases} \dot{\phi}_j = \psi_{j+1} - \psi_j \\ \dot{\psi}_j = \frac{1}{T(\phi_j)}\big[V(\phi_j) - \psi_j + \alpha \cdot (\psi_{j+1} - \psi_j)F(\phi_j)\big] \end{cases} \tag{2}$$

for $j = 1, \dots, N$. Note that, although we consider relative distances (headways) ϕ_j as variables, we do not do the same with relative velocities, keeping absolute velocities ψ_j. This actually simplifies matters in the case of non-constant T (compare to [6]).

Because of the assumptions on function V and of the fact that $\sum_{k=1}^{N} \phi_k = L$, system (2) admits as the only stationary solution $\phi_j^s = L/N$, $\psi_j^s = V(L/N)$ for $j = 1, \dots, N$. Introducing variables $\xi_j = \phi_j - L/N$, $\eta_j = \psi_j - V(L/N)$ for $j = 1, \dots, N$ and $\mathbf{w} = (\xi, \eta)$, the stationary solution becomes $\mathbf{w}^s = \mathbf{0}$. Linearizing around $\mathbf{w}^s = \mathbf{0}$ we find a system of the form $\dot{\mathbf{w}} = \mathbf{M}\mathbf{w}$, where the $2N \times 2N$ matrix $\mathbf{M}$ has the structure

$$\mathbf{M} = \left(\begin{array}{c|c} \mathbf{O}_N & \mathbf{D} \\ \hline \frac{\beta}{\tau}\mathbf{I}_N & \frac{\gamma}{\tau}\mathbf{D} - \frac{1}{\tau}\mathbf{I}_N \end{array}\right) \tag{3}$$

where $\beta = V'(d)$, $\gamma = \alpha F(d)$, $\tau = T(d)$, $\mathbf{I}_N$ is the $(N \times N)$-identity matrix, $\mathbf{O}_N$ is the $(N \times N)$-null matrix and $\mathbf{D}$ is the matrix

$$\mathbf{D} = \begin{pmatrix} -1 & 1 & 0 & \dots & 0 \\ 0 & -1 & 1 & \ddots & \vdots \\ \vdots & \ddots & \ddots & \ddots & 0 \\ 0 & \dots & 0 & -1 & 1 \\ 1 & 0 & \dots & 0 & -1 \end{pmatrix}. \tag{4}$$

The associated characteristic equation is

$$\big[\tau\lambda^2 + (\gamma + 1)\lambda + \beta\big]^N - \big(\gamma\lambda + \beta\big)^N = 0. \tag{5}$$

Notice that $\lambda = 0$ is always an eigenvalue of $\mathbf{M}$ and that this corresponds to the presence of the conserved quantity $\sum_{k=1}^{N} \phi_k = L$. This very relation can be used to reduce the dimension of the system and this needs to be done for two reasons. First we will show below that the system can undergo a Hopf bifurcation but the Hopf theorem cannot be applied when the matrix of the linearized system is singular. Second numerical integration and continuation algorithms greatly gain in stability if no zero eigenvalue is present.

Since the sum of the first N equations of (2) gives $\sum_{k=1}^{N} \dot{\phi}_k = 0$ we can discard the N-th equation and eliminate the only other occurrence of ϕ_N (in the $2N$-th equation) by setting $\phi_N = L - \sum_{k=1}^{N-1} \phi_k$. We obtain the reduced system

$$\begin{cases} \dot{\phi}_j = \psi_{j+1} - \psi_j \qquad j = 1, \ldots, N-1 \\ \dot{\psi}_j = \frac{1}{T(\phi_j)} \big[V(\phi_j) - \psi_j + \alpha \cdot (\psi_{j+1} - \psi_j) F(\phi_j) \big] \quad j = 1, \ldots, N-1 \\ \dot{\psi}_N = \frac{1}{T(L - \sum_{k=1}^{N-1} \phi_k)} \big[V(L - \sum_{k=1}^{N-1} \phi_k) - \psi_N + \alpha \cdot (\psi_1 - \psi_N) F(L - \sum_{k=1}^{N-1} \phi_k) \big] \end{cases} \tag{6}$$

Linearizing system (6), we obtain $\dot{\mathbf{z}} = \mathbf{A}\mathbf{z}$, where $\mathbf{z} := (\phi_1 - d, \ldots, \phi_{N-1} - d, \psi_1 - c, \ldots, \psi_N - c)^T$ and it is easy to show that the $(2N-1) \times (2N-1)$-matrix $\mathbf{A}$ has the same eigenvalues of $\mathbf{M}$ except the zero, i.e., all the solutions of (5) except $\lambda = 0$.

We want to study the stability of the stationary solution when the parameters of the system are varied. The natural candidate as a bifurcation parameter would be N, but it is not suitable for this role because it is discrete and because, varying it, varies the dimension of the system itself. So we fix the value of N and let L vary instead, i.e., we imagine the circuit on which the cars move to shrink or swell. Choosing for example

$$V(x) = \frac{\tanh 2(x-1) + \tanh 2}{1 + \tanh 2}, \quad T(x) = \frac{x^2}{1 + x^2}, \quad F(x) = \frac{0.5}{x + 1},$$

the typical behavior of the eigenvalues of matrix $\mathbf{A}$ (solutions of (5)) can be seen in Figure 1, where we have plotted the curves described by the eigenvalues (in the direction shown by the arrow) as L is increased. For sufficiently small values of L all the eigenvalues have negative real part. Increasing L can cause one or more pairs of eigenvalues to cross the imaginary axis (points A_1 and A_2), so that the stationary solution is unstable and a bifurcation has taken place. A further increase leads once again to a

condition of stability (points B_1 and B_2). Note that in Figure 1 we only drew the $N-1$ eigenvalues that can have a positive imaginary part. There are always N eigenvalues that can never cross the imaginary axis. To study this set $\lambda = i\omega$ in (5) and find solutions $\omega_k = s_k\beta/\sigma_k$ and the conditions for a possible of stability (i.e., the condition for which the k-th couple of eigenvalues is purely imaginary)

$$C_k(\frac{L}{N}) := \frac{\tau\beta}{\sigma_k^2} - \frac{\gamma}{\sigma_k} = \frac{1}{1+c_k}, \tag{7}$$

for $k = 1, \ldots, N-1$, where $c_k := \cos(2\pi k/N)$, $\sigma_k := 1-\gamma(c_k-1)$. Note that the left hand side of (7) depends on L/N through γ, τ and β, while the right hand side only depends on N. As we will show, the only bifurcation that produces stable periodic solutions is the one corresponding to $k = 1$, which is drawn in Figure 2. The intersection points L_1^H and L_2^H correspond to the two crossings of the imaginary axis described above. Note that function C_1 is bell-shaped due to the assumptions made on the functions V, T and F.

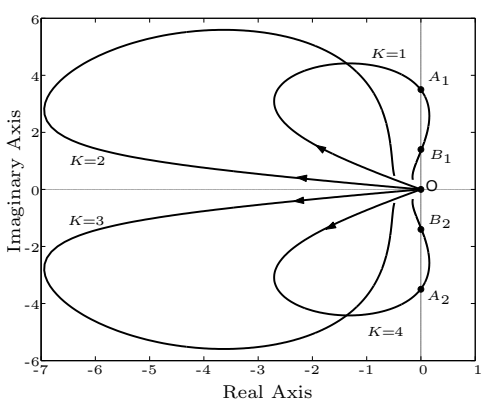

Figure 1. Four of the nine eigenvalues for five cars ($N = 5$). The remaining five eigenvalues are not drawn and do not affect the stability.

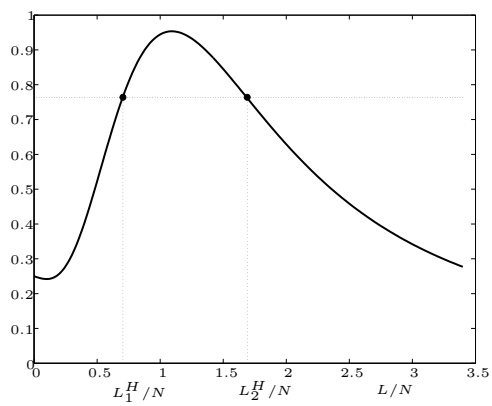

Figure 2. The $C_1(\frac{L}{N})$ curve and the line $y=(1+\cos\frac{2\pi}{N})^{-1}$ for $N=5$.

This suggests that for $L = L_{1,2}^H$ the system undergoes a Hopf bifurcation and therefore periodic orbits will appear (at least locally).

Theorem 1. *If N is fixed and $L = L^H$ is such that*

$$C_1(\frac{L^H}{N}) = \frac{1}{1+\cos\frac{2\pi}{N}} \tag{8}$$

holds, then system (6) *undergoes a Hopf bifurcation.*

Proof. If (8) is verified for some L^H, there is a solution of (5) $\lambda_1 := \lambda_1(L) := \mu_1(L) + i\omega_1(L)$ such that $\mu_1(L^H) = 0$. It is sufficient to prove that $\mu'(L^H) \neq 0$. This is true and it can be directly checked as in [6]. □

Remark 1. It is possible to calculate the first Lyapunov coefficient of the bifurcation $\ell_1(L)$ (again see [6] for an example of such calculation and [16] for the underlying theory) and, if $\ell_1(L^H) \neq 0$, this can be used to gain insight in the stability of the generated periodic solutions, i.e., in sub- or super-criticality of the bifurcation.

In the next section we show that this is the case. Note that to rigorously state that we are indeed observing a Hopf bifurcation for $L = L^H_{1,2}$ two genericity conditions must be verified. These involve long and tedious calculations, especially those relative to the Lyapunov coefficient, and are not reported here. For an example on how to proceed see [6].

Let us discuss another aspect of the conditions (7). Considering $\tau = \tau(L, N, \alpha)$ we can solve equation (7) for τ

$$\tau(L, N, \alpha) = \frac{(1+2\alpha F(\frac{L}{N}))[1+\alpha F(\frac{L}{N})(1-\cos\frac{2\pi}{N})]}{V'(\frac{L}{N})(1+\cos\frac{2\pi}{N})} \tag{9}$$

For fixed N and α this is a function of L such that $\lim_{L\to 0^+} = \lim_{L\to\infty} = \infty$. In addition we have $\frac{\partial\tau}{\partial\alpha} > 0, \quad \forall L, N$. This can be summarized in the following lemma.

Lemma 1. *Aggressive driving behavior increases the stability* (*of the quasi-stationary solutions*) *in the sense that*

$$\frac{\partial\tau}{\partial\alpha} > 0, \quad \forall L, N.$$

The result of this lemma can be interpreted in two ways. The loss of stability occurs for fixed L and increasing α at higher values of τ. Alternatively we can say, that for fixed τ and increasing α the unstable region (in values

of L) becomes smaller. Note that, though aggressive drivers reduce the occurrence of traffic jams, they might induce more car crashes. In fact there are investigations, where on one hand a stabilizing effect of aggressiveness and on the other hand an increased crash risk are observed [20].

2. Numerical Bifurcation Analysis

In this section we want to solve system (6) numerically with `AUTO2000` (see [5]) to understand its global behavior. It is our special concern to show the dependence on different reaction times $T(x)$ and on parameter α that corresponds to the aggressiveness of the drivers. Various bifurcation diagrams will be drawn with L on the x-axis and a special norm of the solution

$$\text{Norm}(x) := \sqrt{\int_0^1 \big[\sum_{j=1}^{N-1} \phi_j(t)^2 + \sum_{k=1}^{N} \psi_j(t)^2 \big] dt} \tag{10}$$

on the y-axis with $\mathbf{x} = (\phi_1, \ldots, \phi_{N-1}, \psi_1, \ldots, \psi_N)^T$. In case of the stationary solution Eq. (10) becomes

$$\text{Norm}(x) := \sqrt{\sum_{j=1}^{N-1} \left(\frac{L}{N}\right)^2 + \sum_{j=1}^{N} V\left(\frac{L}{N}\right)^2},$$

which is drawn in Figure 3(a).

We always choose $F(x) = 0.5(x+1)^{-1}$ for the numerical analysis and use $V(x) = V_{max}\frac{x^2}{1+x^2}$ as an optimal velocity function (see [18]).

2.1. Aggressive drivers with constant reaction time

Let us examine the effect of the aggressive term with constant reaction times, i.e., we set $T = 1$ in (6). A typical bifurcation diagram for this case is drawn in Figure 3(b). What we see is the stationary solution that becomes unstable on the left (with label 1) and then stable on the right Hopf bifurcation point (label 2). These two Hopf points are joined by a branch of periodic solutions, the labels 5, 6 and 7 correspond to period doubling points, label 4 to a fold. In Figure 4(a)we see solution 3 where all the five headways between the drivers are plotted as a function of time. One can

see that the solution is a traveling wave with a phase shift of $\frac{1}{5}$ (the time is always scaled with respect to the period of the solution under consideration).

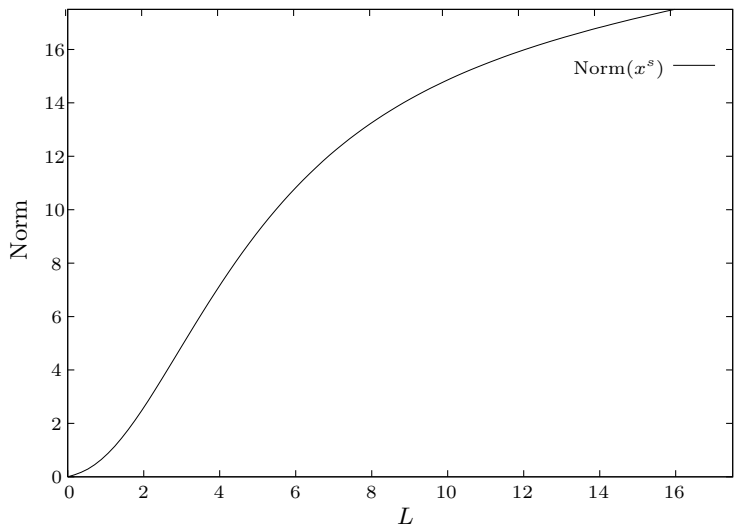

(a) Norm of the stationary solution.

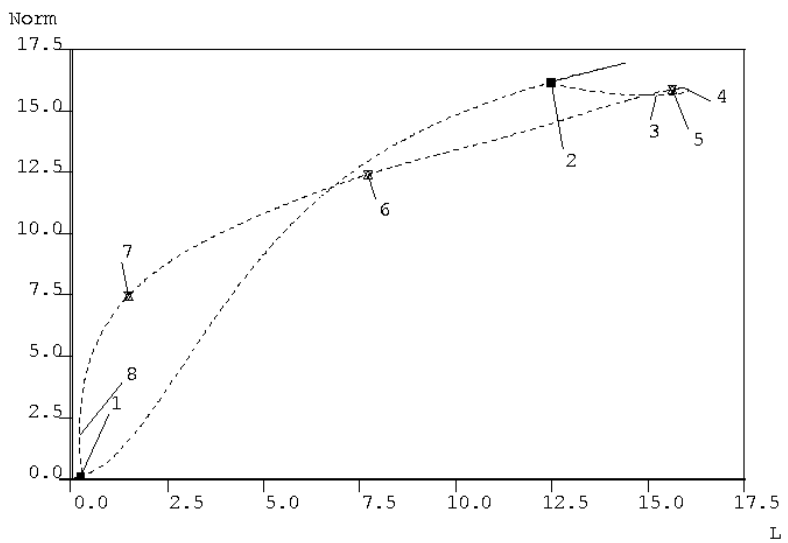

(b) Two Hopf bifurcation points (1 and 2) joined by a branch of periodic solutions.

Figure 3. Two Bifurcation diagrams for $N = 5$, $V^{max} = 8$ and a function $T(x) = 1$.

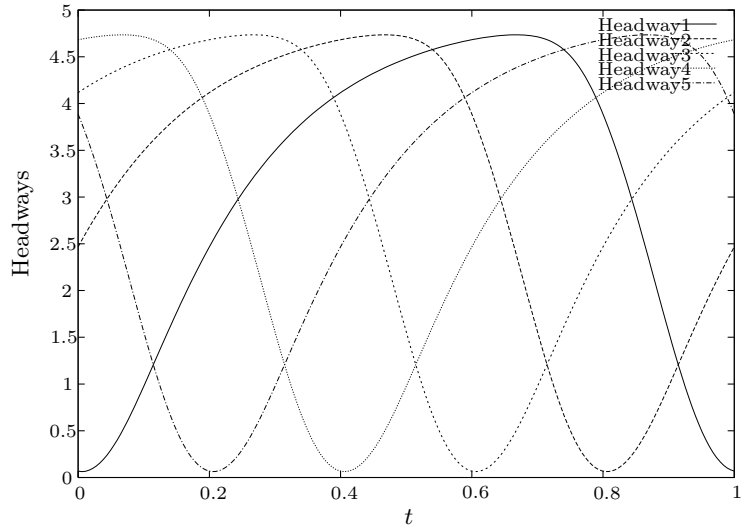

(a) The traveling wave solution corresponding to label 3 in Figure 3(b).

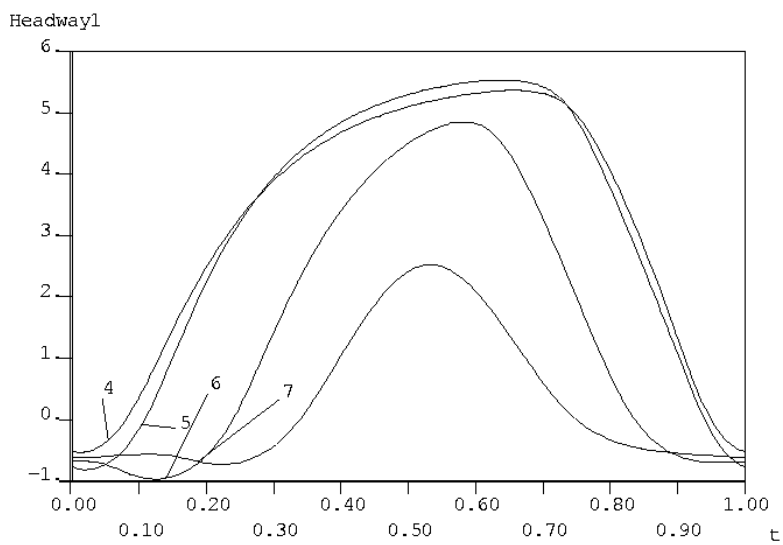

(b) The *unphysical* solutions corresponding to labels 4, 5, 6 and 7 in Figure 3(b) (one car each).

Figure 4. Bifurcation diagram and a periodic solution for $N = 5$, $V^{max} = 8$ and a function $T(x) = 1$.

As mentioned before, there are two main aspects which need to be taken into account: the stability and the physicality of both stationary and peri-

odical solutions. In fact most periodical solutions in Figure 3(b) (e.g., see Figure 4(b) are *unphysical* (negative headways).

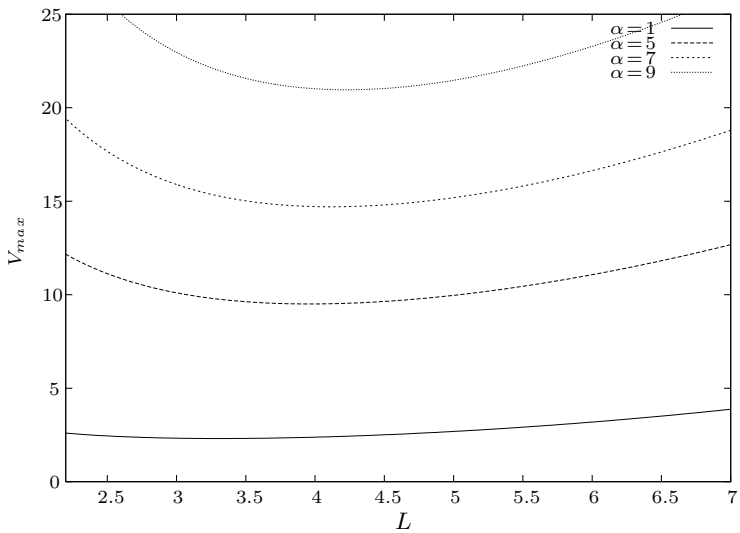

Figure 5. (L, V_{max})-diagram with varying α for $N = 5$ and with (constant) function $T(x) = 1$.

Figure 5 shows the influence of α on the stability of the stationary solution. The L/V_{max}-diagram shows the manifolds of the Hopf bifurcation points with varying α as a numerical result from calculations with `AUTO2000`. According to Lemma 1 the Hopf curve moves upward (in positive V_{max} direction) as α is increased, which means that the region in parameter space, where the stationary solution is stable, grows.

2.2. The pure optimal velocity model with variable reaction time ($\alpha = 0$)

In the previous section we always chose the reaction time $T(x) = 1$. Now we want to have a look at the influence of a non-constant T on the bifurcation diagrams. In the simulations that correspond to Figures 6 and 7(a) T is still constant but very small. One can see, that in the first case ($T(x) = 0.1$) there is no unstable stationary solution while in the second ($T(x) = 0.2$) the distance between the two Hopf bifurcation points, that are joined by a branch of stable periodic solutions, is small. This is what we would expect from real traffic: drivers who are quicker to react, can better

absorb perturbations and find again the ordered situation corresponding to the stationary solution.

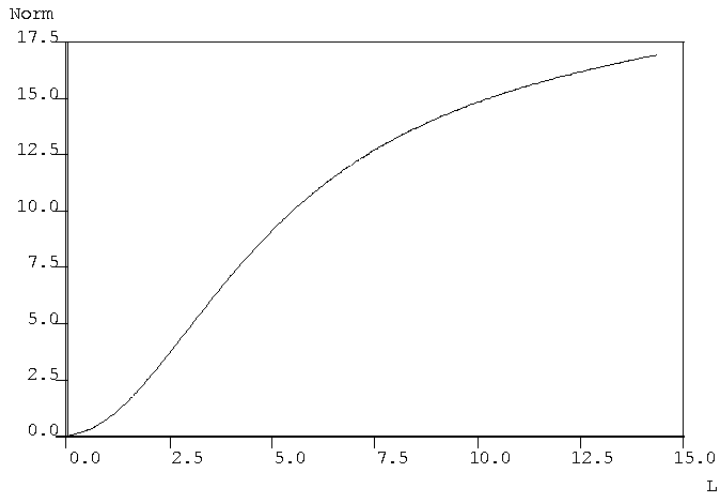

Figure 6. Bifurcation diagram for $N = 5$, $V_{max} = 8$ and constant (low) $T(x) = 0.1$.

From Figure 7(b) it can be seen that there are still unrealistic periodic solutions in the simulation because the headways are sometimes negative.

Next we would like to combine the previous reaction times by taking a function T that is 0.2 for small headways and 1 for big ones. This seems to be a realistic approach, because drivers become more attentive when they are closer to the car ahead.

Figure 8 shows the results of the simulation with $T_1(x) = \frac{x^2}{1+x^2}0.8 + 0.2$. Again in Figure 8(a), we see two Hopf bifurcation points (1, 2), two period doubling points (7, 10) and further on two folds (5,6). The area with stable periodic solutions is bigger than in Figure 4 but Figure 8(b) shows that solutions 8, 9, 10 are still unphysical while only the headways of solution 4 stay positive (we plotted just one headway as the solutions are always traveling waves).

In comparison to this see Figure 9 where we use the function $T_2(x) = \frac{x^6}{1+x^6}0.8 + 0.2$ as a reaction time with a faster changeover between the two different states than T_1. It can be recognized from that the headways corresponding to solutions 3, 4, 5 and 6 in Figure 9(b) are positive, so it looks like the new reaction time works like a bumper between the cars.

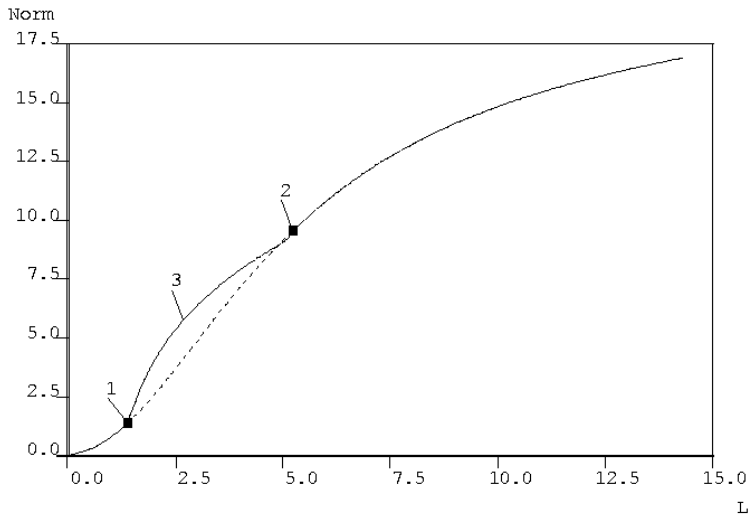

(a) Bifurcation diagram.

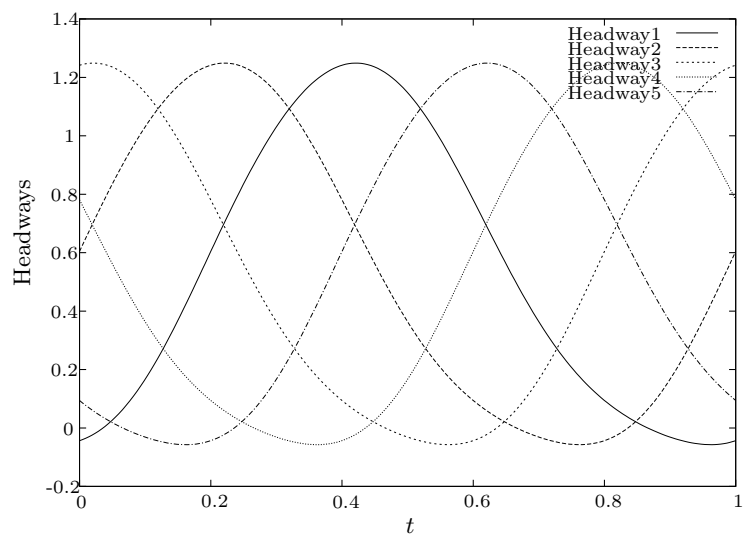

(b) The traveling wave corresponding to the (unphysical) solution 3 in Figure 7(a).

Figure 7. Bifurcation diagram and a special periodic solution for $N = 5$, $V_{max} = 8$ and constant (low) $T(x) = 0.2$.

In Figure 10 three different reaction times T_1, T_2 and T_3 can be seen where in T_3 the drivers are more watchfully for small headways than in T_1 and T_2.

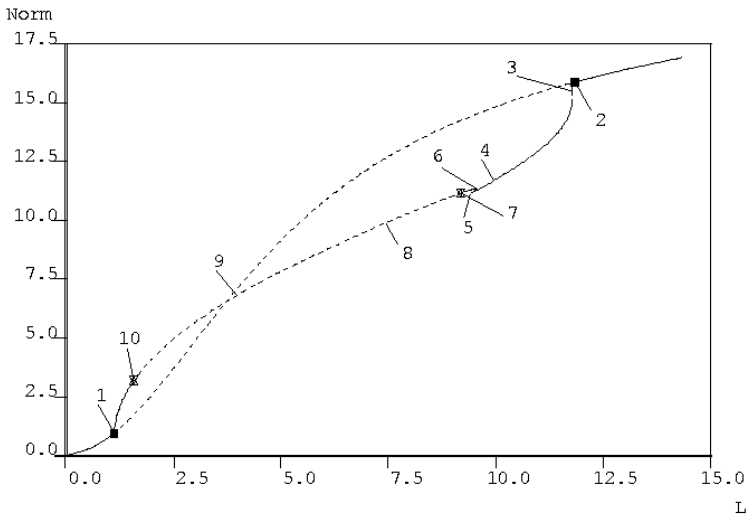

(a) Two Hopf bifurcation points joined by a branch of periodic solutions.

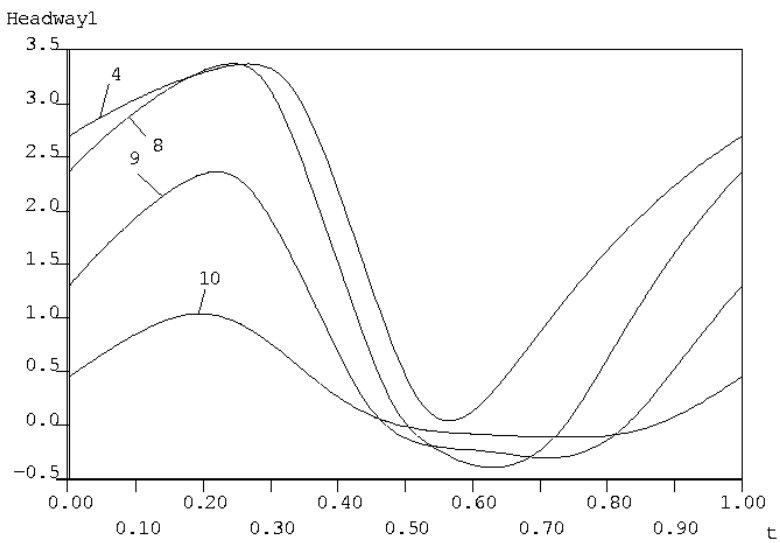

(b) Solutions corresponding to labels 4, 8, 9 and 10 in Figure 8(a) projected into the evolution in time of the headway between the first two drivers.

Figure 8. Bifurcation diagram and periodic solutions for $N = 5$, $V^{max} = 8$ and a function $T_1(x) = \frac{x^2}{1+x^2}0.8 + 0.2$.

At last we want to increase the number of cars in order to see if the system behaves in a similar way as before. Therefore we choose the function

$T_3(x) = \frac{x^6}{1+x^6}0.9 + 0.1$ as reaction time and repeat the previous simulation with ten cars.

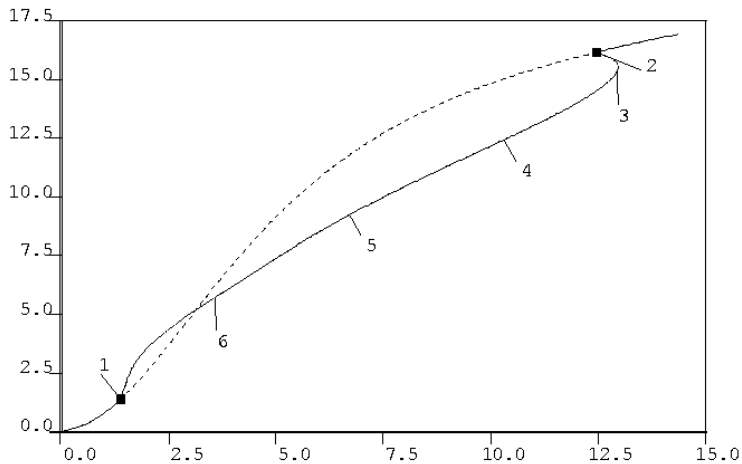

(a) Two Hopf bifurcation points joined by a branch of periodic solutions.

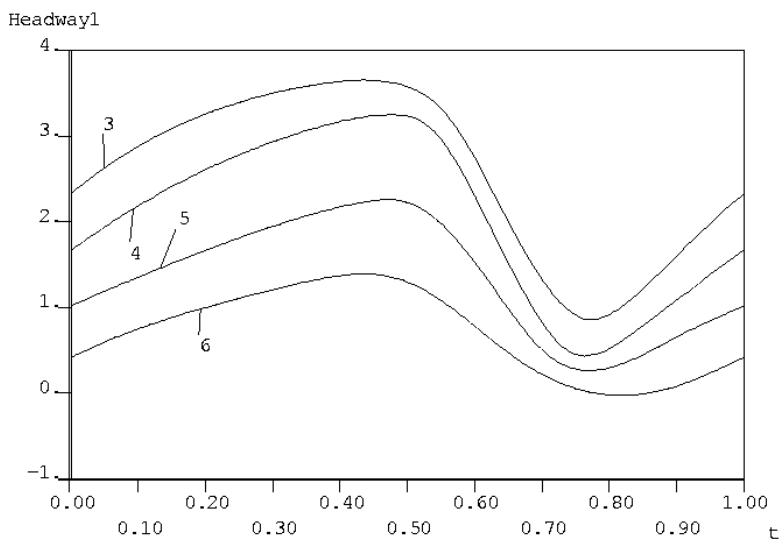

(b) Solutions corresponding to labels 3 to 6 in Figure 9(a).

Figure 9. Bifurcation diagram and phase space portrait of a periodic solution for $N = 5$, $V^{max} = 8$ and a function $T_2(x) = \frac{x^6}{1+x^6}0.8 + 0.2$.

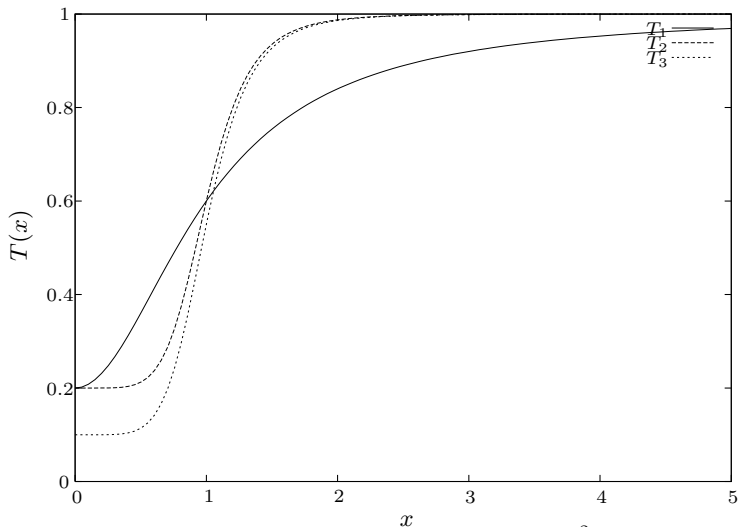

Figure 10. Three different functions $T_1(x) = \frac{x^2}{1+x^2}0.8 + 0.2$, $T_2(x) = \frac{x^6}{1+x^6}0.8 + 0.2$ and $T_3(x) = \frac{x^6}{1+x^6}0.9 + 0.1$.

The bifurcation diagram and the phase space in Figure 11 affirm the results from before. We now have six Hopf bifurcations (with labels 1 to 6) from which the outer, where the stationary solutions changes its stability,

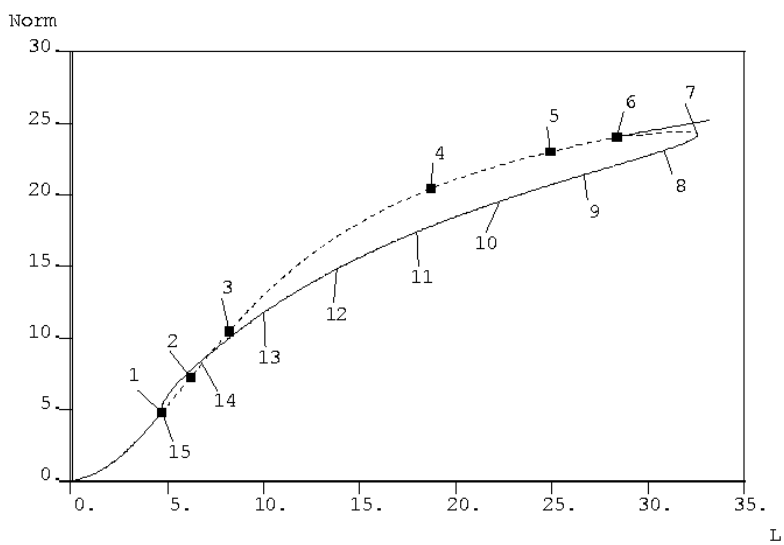

(a) Two Hopf bifurcation points joined by a branch of periodic solutions.

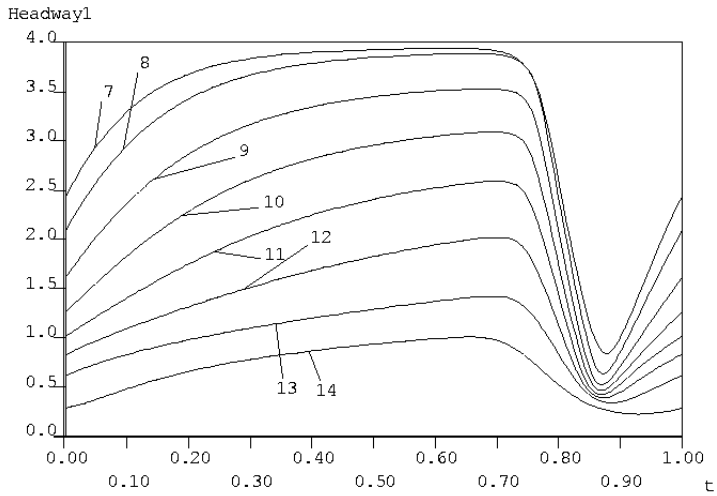

(b) Solutions corresponding to labels 7 to 14 in Figure 11(a).

Figure 11. Bifurcation diagram and periodic solutions for $N = 10$, $V^{max} = 8$ and a reaction time $T_3(x) = \frac{x^6}{1+x^6}0.9 + 0.1$.

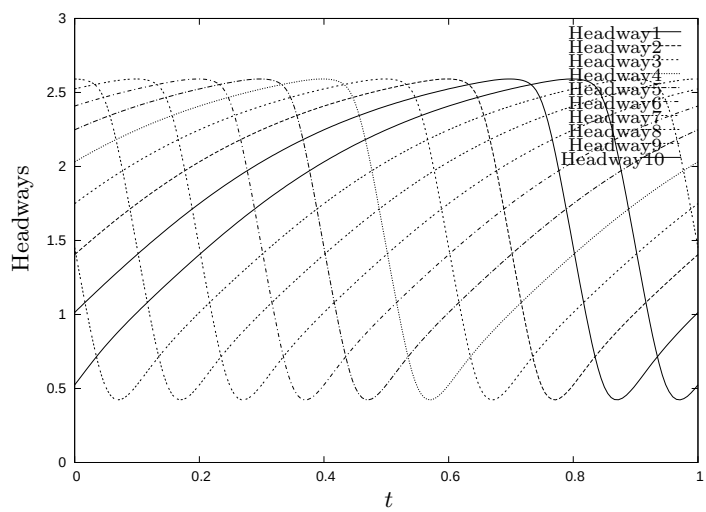

Figure 12. Traveling wave solution corresponding to label 11 in Figure 11(a).

are the most interesting ones. Between them, the branch of periodic solutions becomes stable after a fold (solution 7). Figure 12 shows the traveling wave of solution 11 where the ten headways of the drivers contain a phase shift of $\frac{1}{10}$ over the whole period now. There is no orbit in the branch of periodic

solutions between the Hopf bifurcations that is unrealistic (Figure 11(b)).

2.3. The full model (1)

In this final subsection we use both the variable reaction time T and the aggressiveness of the drivers α for parameters that might have an influence of the stability and the quality of the system concerning the unrealistic solutions. Figures 13 and 14 show the effect of these two quantities.

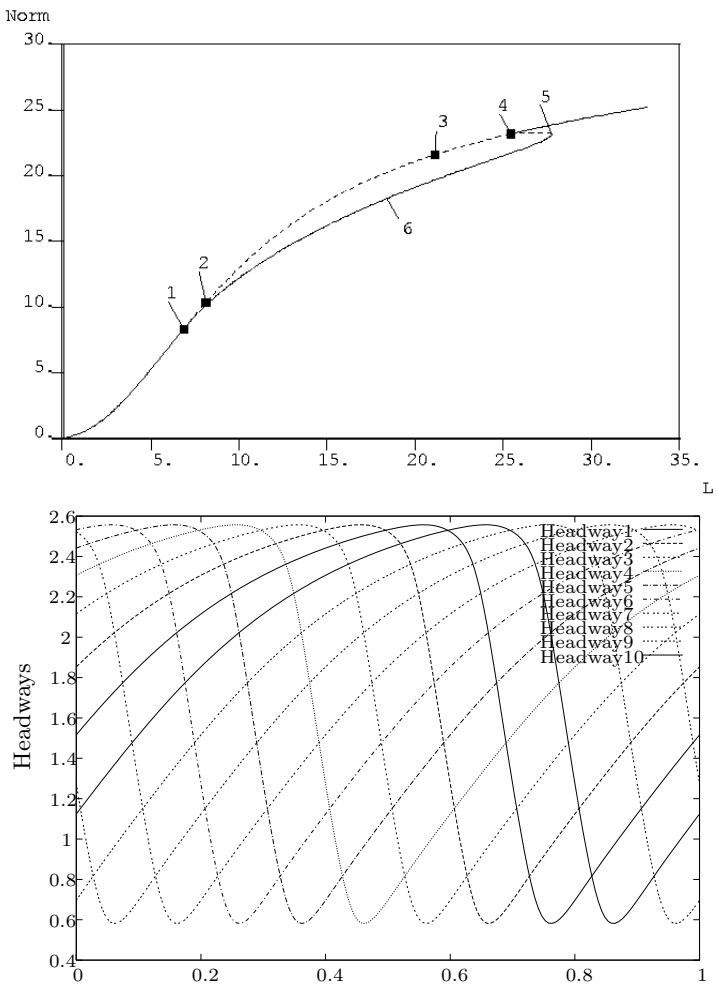

(b) Traveling wave corresponding to label 6 in Figure 13(a).

Figure 13. Bifurcation diagrams and phase space portrait of some periodic solutions with $\alpha = 1$. $N = 10$, $V^{max} = 8$ and a function $T_3(x) = \frac{x^6}{1+x^6} 0.9 + 0.1$.

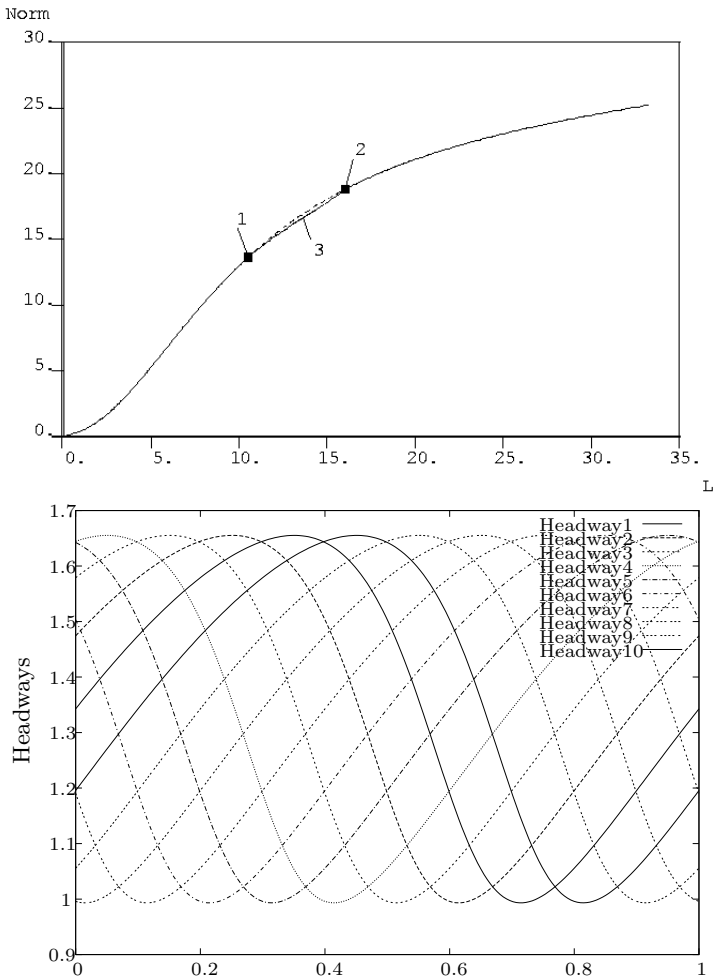

(b) Traveling wave corresponding to label 3 in Figure 14(a).

Figure 14. Bifurcation diagrams and phase space portrait of some periodic solutions with $\alpha = 5$. $N = 10$, $V^{max} = 8$ and a function $T_3(x) = \frac{x^6}{1+x^6} 0.9 + 0.1$.

One can directly compare Figure 13(a) and 14(a) to Figure 11 (where $\alpha = 0$). First we know from subsection 2.1 and from the theoretical analysis, that an increasing α makes the system more stable in the sense explaned above. But this implicates that for a fixed V_{max} the distant between the two outer Hopf bifurcation points shrinks. Hence the bifurcating periodic solutions have a decreasing amplitude. Further more one can see from Figures 11(b), 13(b) and 14(b) that the minimum of the particular traveling wave increases – in a way the solutions become more realistic.

Conclusions

This paper is step forward to explore the dynamics of simple follow the leader models. Apparently even the simplest models seem to describe already very interesting dynamical phenomena. We plan to further investigate these models and to explore even more complicated phenomena like the already observed period doublings.

Acknowledgments

The first author was partially supported by the European IHP-Network *HYKE: Hyperbolic and Kinetic Equations* (contract number: HPRN-CT-2002-00282). The third author was supported by the Graduiertenkolleg *Erhaltungsprinzipien in der Modellierung und Simulation mariner, atmosphärischer und technischer Systeme* (GrK number 431) of the *Deutsche Forschungsgemeinschaft.*

References

1. M. Bando, K. Hasebe, K. Nakanishi and A. Nakayama, Analysis of an optimal velocity model with explicit delay, *Phys. Rev. E*, **58**(1998), 5429.

2. M. Bando, K. Hasebe, A. Nakayama, A. Shibata and Y. Sugiyama, Structure stability of congestion in traffic dynamics, *Japan. J. Indust. Appl. Math.*, **11**(1994), 203.

3. M. Bando, K. Hasebe, A. Nakayama, A. Shibata and Y. Sugiyama, Dynamical model of traffic congestion and numerical simulation, *Phys. Rev. E*, **51**(1995), 1035.

4. M. Brackstone and M. McDonald, Car Following: A Historical Review, *Transp. Res. F*, **2**(2000), 181.

5. E. J. Doedel, R. C. Paffenroth, A. R. Champneys, T. F. Fairgrieve, Yu. A. Kuznetsov, B. Sandstede and X. Wang, AUTO 2000: Continuation and bifurcation software for ordinary differential equation (with HomCont), Tech. Rep., Caltech, 2001.

6. I. Gasser, G. Sirito and B. Werner, Bifurcation analysis of a class of 'car following' traffic models, *Phys. D*, **197**(2004), no.3-4, 222-241.

7. D. C. Gazis, R. Herman and R. W. Rothery, Nonlinear follow the leader models of traffic flow, *Oper. Res.*, **9**(1961), 545-567.

8. J. M. Greenberg, Traffic Congestion - An Instability in a Hyperbolic System, submitted to *Transport Theory Statist. Phys.*, (2005).

9. D. Helbing, *Verkehrsdynamik*, Springer, 1997.

10. D. Helbing, Traffic and Related Self-Driven Many-Particle Systems, *Rev. Modern Phys.*, **73**(2001), 1067-1141.

11. H. J. C. Huijberts, Improved stability bound for steady state flow in a car-following model of road traffic on a circular road, *Phys. Rev. E*, **65**(2002).

12. H. J. C. Huijberts, Analysis of a continuous car-following model for a bus route: existence, stability and bifurcation of synchronous motions, *Phys. A*, **308**(2002), 489-517.

13. Y. Igarashi, K. Itoh, K. Nakanishi, K. Ogura and K. Yokokawa, Bifurcation phenomena in the optimal velocity model for traffic flow, *Phys. Rev. E*, **64**(2001).

14. R. Illner, A. Klar and T. Materne, Vlasov-Fokker-Planck models for multilane traffic Flow, *Comm. Math. Sci.*, **1**(2003), no.1, 1-12.

15. A. Klar, R. D. Kühne and R. Wegener, Mathematical models for vehicular traffic, *Surv. Math. Ind.*, **6**(1996), 215-239.

16. Y. A. Kuznetsov, *Elements of Applied Bifurcation Theory*, Springer, 1998.

17. M. J. Lighthill and G. B. Whitham, A theory of traffic flow on long crowded roads, *Proc. Roy. Soc. A*, **229**(1955), 317-345.

18. R. Mahnke and N. Pieret, Stochastic master-equation approach to aggregation in freeway traffic, *Phys. Rev. E*, **55**(1997), 2203.

19. A. D. Mason and A. W. Woods, Car-following model of multispecies systems of road traffic, *Phys. Rev. E* **55**(1997), 2203.

20. L. E. Olmos and J. D. Munoz, A cellular automaton model for the traffic flow in Bogota, *Internat. J. Modern Phys. C*, (2004), 0406065.

21. G. Orosz, R. E. Wilson and B. Krauskopf, Global bifurcation investigation of an optimal velocity traffic model with driver reaction time, *Phys. Rev. E*, **70**(2004), no.2, 026207, 1-10.

22. L. A. Pipes, An operational analysis of traffic dynamics, *J. Appl. Phys.*, **24**(1953), 274.

23. A. Reuschel, Fahrzeugbewegungen in der Kolonne, *Österr. Ing.-Archiv*, **4**(1950), 193.

Universität Hamburg, Fachbereich Mathematik, Bundesstraße 55, 20146 Hamburg, Germany.
E-mail: gasser@math.uni-hamburg.de

Universität Hamburg, Fachbereich Mathematik, Bundesstraße 55, 20146 Hamburg, Germany.
E-mail: seidel@math.uni-hamburg.de

Universität Hamburg, Fachbereich Mathematik, Bundesstraße 55, 20146 Hamburg, Germany.
E-mail: sirito@math.uni-hamburg.de

Universität Hamburg, Fachbereich Mathematik, Bundesstraße 55, 20146 Hamburg, Germany.
E-mail: werner@math.uni-hamburg.de